Available online at www.sciencedirect.com

Food and Bioproducts Processing

journal homepage: www.elsevier.com/locate/fbp

A comparison of vegetable leaves and replicated biomimetic surfaces on the binding of *Escherichia coli* and *Listeria monocytogenes*

Luciana C. Gomes[a,b], *Fabien Saubade*[c], *Moshin Amin*[c], *Joshua Spall*[c], *Christopher M. Liauw*[c], *Filipe Mergulhão*[a,b], *Kathryn A. Whitehead*[c,*]

[a] *LEPABE - Laboratory for Process Engineering, Environment, Biotechnology and Energy, Faculty of Engineering, University of Porto, Rua Dr. Roberto Frias, 4200-465 Porto, Portugal*

[b] *ALiCE - Associate Laboratory in Chemical Engineering, Faculty of Engineering, University of Porto, Rua Dr. Roberto Frias, 4200-465 Porto, Portugal*

[c] *Microbiology at Interfaces, Manchester Metropolitan University, Chester Street, Manchester M1 5GD, UK*

ARTICLE INFO

Article history:
Received 15 July 2022
Received in revised form 21 October 2022
Accepted 8 November 2022
Available online 11 November 2022

Keywords:
Biomimetic surfaces
Leaves
Food industry
Biofouling
Escherichia coli
Listeria monocytogenes

ABSTRACT

Biofouling in the food industry is a huge issue, and one possible way to reduce surface fouling is to understand how naturally cleaning surfaces based on biomimetic designs influence bacterial binding. Four self-cleaning leaves (Tenderheart cabbage, Cauliflower, White cabbage and Leek) were analysed for their surface properties and artificial replicates were produced. The leaves and surfaces were subjected to attachment, adhesion and retention assays using *Escherichia coli* and *Listeria monocytogenes*. For the attachment assays, the lowest cell numbers occurred on the least hydrophobic and smooth surfaces but were higher than the flat control surface, regardless of the strain. Following the adhesion assays, using *L. monocytogenes*, the Tenderheart and Cauliflower biomimetic replicated leaves resulted in significantly lowered cell adhesion. Following the retention assays, White cabbage demonstrated lower cell retention for both types of bacteria on the biomimetic replicated surface compared to the flat control surface. The biomimetic surfaces were also more efficient at avoiding bacterial retention than natural leaves, with reductions of about 1 and 2 Log in *L. monocytogenes* and *E. coli* retention, respectively, on most of the produced surfaces. Although the surfaces were promising in reducing bacterial binding, the results suggested that different experimental assays exerted different influences on the conclusions. This work demonstrated that consideration needs to be given to the environmental factors where the surface is to be used and that bacterial species influence the propensity of biofouling on a surface.

1. Introduction

Biofilms formed by foodborne pathogens that occur in and on food industry equipment are a major problem since they are a frequent source of product contamination, resulting in economic losses for processors and posing serious health concerns for consumers (Chmielewski and Frank, 2003). Safer food production may entail high cleaning costs and severe environmental impacts (such as water and energy consumption, wastewater production, and increasing bacterial resistance to antimicrobial agents) to reduce contamination (Moreira et al., 2016). Therefore, the development of new antifouling strategies focused on preventing bacterial

* Corresponding author.
E-mail address:
K.A.Whitehead@mmu.ac.uk (K.A. Whitehead).

https://doi.org/10.1016/j.fbp.2022.11.003

colonization and biofilm formation instead of their elimination is very promising for the industrial sector.

Surface modification to prevent contamination is a key topic of research and several different approaches have been developed (Matinha-Cardoso et al., 2021; Rajab et al., 2017; Silva et al., 2021; Vorobii et al., 2022). One solution has been the development of biomimetic superhydrophobic surfaces, which have shown great potential applications in many fields, including (1) the marine sector to minimize the settlement of marine organisms on boats, ports and any infrastructure kept in the sea for some time (Chen et al., 2021), (2) the biomedical field in tissue engineering approaches, and against bacteria and blood components (Damodaran and Murthy, 2016; Monteiro et al., 2022), and (3) food packaging and food facility scenarios to take advantage of the water-repellency and anti-icing capabilities of biomimetic coatings (Alon et al., 2022; Lazzini et al., 2017; Zouaghi et al., 2019). Particularly in the food area, the combination of chemical and physical structures of biomimetic surfaces has been explored for post-harvest packaging materials (Alon et al., 2022) and industrial pasteurization equipment (Zouaghi et al., 2019; Zouaghi et al., 2017) in order to inhibit fouling. More recently, biomimetic surfaces with superwettability have been proposed to delay icing and frosting on cold substrates or to de-ice and de-frost easily, with the potential of supplementing or even replacing conventional de-icing or defrosting technologies in the food industry (Zhu et al., 2021). Additionally, biomimetic biosensors mimicking the porous media of fresh produce have been studied to detect the presence of bacteria in low concentration, monitor their internalization, and also evaluate the potential formation of biofilm (Arreguin-Campos et al., 2021; Huffman et al., 2017).

One of the most well-known biomimetic surfaces that has been replicated using a number of different engineering approaches is the superhydrophobic lotus-like surface, which presents self-cleaning abilities due to its particular wetting regime (Moerman, 2014). Although most leaves appear smooth to the naked eye, under a microscope, from a microbiological perspective, their surfaces contain a huge number of macro- (> 5 μm), micro- (≤ 5–0.5 μm), and nano-scale (≤ 0.5 μm) papillae and structures that are coated in a hydrophobic wax. This hierarchical structure in which the macro- and micro-scale surface features have nano-scale roughness contributes to the hydrophobic properties of the surface, reducing the area on which water, debris and microorganisms can attach (Moerman, 2014). A wide range of engineering approaches has been used to try to replicate such surfaces. These include complex methods such as using a soft lithography technique on stainless steel plates to reproduce the surface properties of leaves from *Colocasia esculenta, Crocosmia aurea,* and *Salvinia molesta* (Arango-Santander et al., 2021), and nanosecond laser technology on titanium alloy to produce titania nano petals or nanorod layers (Li et al., 2013). However, there has been an increasing interest in reproducing the surface properties of biomimetic surfaces using simpler methodologies. These have included reproducing the leaves of lotus and rice on gold surfaces using polydimethylsiloxane (PDMS), and then chemically modifying them with alkanethiol (Zhao et al., 2010), recreating two bamboo varieties and *Gi0nkgo biloba* using a PDMS replicating protocol (Legrand et al., 2021), reproducing the morphology and wettability of water bamboo leaves using PDMS (Guan et al., 2015), and replicating the surface of the *Gladiolus hybridus* (Gladioli) leaf using silicone material to create a negative mould of the leaf surface, followed by using dental wax to produce a biomimetic surface (McClements et al., 2021).

The recreation of the properties of biomimetic surfaces is complex. A superhydrophobic surface typically has an apparent water contact angle (CA) greater than 150° and small CA hysteresis (Ramachandran et al., 2015). It has been suggested that the superhydrophobic properties of the surface can be influenced by the surface structure and material composition (Peng et al., 2013). However, it has also been shown that surfaces can exhibit a high contact angle coupled with either low or high adhesion by virtue of surface topography alone (Peng et al., 2013). Some superhydrophobic surfaces have been shown to have a high CA and, at the same time, strong adhesion with water and, therefore, large CA hysteresis, a phenomenon that was called 'rose petal effect' (Ramachandran et al., 2015). Both types of surfaces may be replicated and adapted to understand the interactions between the surfaces, biofouling and interfacial phenomena. One key area where superhydrophobic surfaces that repel water could be extremely useful is in the food industry to reduce bacterial binding to surfaces. For example, Zouaghi et al. (2017) produced slippery liquid-infused surfaces inspired by the Nepenthes pitcher plant on food-grade stainless steel via femtosecond laser ablation, followed by fluorosilanization and impregnation with an inert perfluorinated oil. These authors demonstrated that no trace of dairy deposit was found after 90 min of pasteurization test in pilot-scale equipment followed by a short water rinse.

Two of the most important pathogens that occur in the food industry are *Listeria monocytogenes* and *Escherichia coli*. Both are opportunistic foodborne pathogens: *L. monocytogenes* is the causative agent of listeriosis, whilst *E. coli* is found in water and food, and can cause foodborne disease (de Grandi et al., 2018; Klayman et al., 2009). Bacterial attachment, adhesion, and retention are a pre1requisite for biofilm formation, and such issues can lead to poor hygienic conditions in food processing environments (Røder et al., 2015).

In this work, surfaces were replicated to utilise the antifouling properties that occur naturally on the surfaces of plant leaves. The aim of this study was to replicate the self-cleaning surfaces of cabbages - *Brassica oleracea* (Tenderheart), *Brassica oleracea capitate* (White cabbage), *Brassica oleracea var. botrytis* (Cauliflower), and *Allium ampeloprasu* (Leek) - using a casting technique. Negative silicone moulds of the leaves surfaces were manufactured and dental wax was used to create the biomimetic surfaces because it is a low-cost, easily mouldable material, and mimics the crystalline hydrocarbons found on several hydrophobic leaves (McClements et al., 2021). The biomimetic wax surfaces were then compared with the original leaves and flat wax surface (control) to determine the effectiveness of plant-based surfaces in counteracting bacterial attachment, adhesion and retention. In this instance, bacterial attachment was defined as the initial stage of interaction between bacterial cells and the surface, and is followed by adhesion (stronger chemical bonds between surface-bacteria), and finally retention on a surface (the final step before biofilm formation) (Rajab et al., 2018). These results help to understand how mimicking the topography of a self-cleaning leaf and testing using a range of bacterial binding methodologies can impact the antifouling behaviour of a replicated biomimetic surface.

2. Materials and methods

2.1. Production of biomimetic surfaces

To fabricate biomimetic replicates, several biological samples of the same leaf type were mounted with double-sided tape on a smooth surface and an addition-cured silicone duplicating system (Shera Duo-Sil H, Shera GmbH & Co. KG, Germany) was poured on the adaxial surfaces of the leaves in order to produce a negative mould. Dental wax (Kemdent Eco dental wax, UK) was then poured onto the negative mould, creating a positive wax surface for each leaf (McClements et al., 2021). A 15 mm diameter steel hole punch was used to create equally sized coupons.

2.2. Surface characterization

The brassica leaves and leek, together with the biomimetic and flat wax surfaces, were characterized regarding the water contact angle and surface hydrophobicity (using drop goniometer), roughness (by Optical Profilometry, OP), morphology (using Scanning Electron Microscopy, SEM), and chemistry (using Attenuated Total Reflection – Fourier Transform Infrared Spectroscopy, ATR-FTIR).

2.2.1. Scanning electron microscopy (SEM)

The original leaves and biomimetic wax surfaces were soaked for 24 h at 4 °C in 4 % (v/v) glutaraldehyde (Agar Scientific, UK), washed with sterile water, dried overnight, and finally stored in a desiccator until visualisation to remove any trace of water from almost-dry samples. The samples were then fixed (adaxial side up) to SEM stubs using carbon pads (Agar Scientific, UK) and sputter-coated with gold in an SEM coating system (Polaron, UK). The sputter coating conditions were: 5 mA (plasma current), pressure < 0.1 mbar, 800 V, and argon gas for 30 s. The secondary electron detector of a Supra 40VP scanning electron microscope (Carl Zeiss Ltd., UK) was used to obtain the images at an accelerating voltage of 2 kV and a magnification of 5000 × .

2.2.2. Optical Profilometry (OP)

The surface roughness of the leaves and wax replicates were evaluated using a MicroXAM (phase-shift) surface mapping microscope (ADE Corporation, XYZ model 4400 mL system, USA) with an AD phase-shift controller (Omniscan, UK). Each analysis was carried out using extended-range vertical scanning interferometry, and the MAPVIEW AE 2.17 (Omniscan, UK) image analysis system was utilized to extract the root-mean-square roughness (S_q) and peak to valey height (S_{pv}) (n = 9) (Skovager et al., 2013).

2.2.3. Water contact angle and surface hydrophobicity

The surface-energy components of the leaves and replicates were calculated according to the work by van Oss and colleagues (van Oss, 1995), which considers the contact angles of three test liquids including water to estimate the interfacial free energy (ΔG_{iwi}). The contact angles of each surface were determined using a drop goniometer (GH11 model, Krüss, France) and a PC-based data analysis system as described in McClements et al. (2021). The interfacial free energy was used as a measure of the hydrophobicity of a surface where greater (negative) ΔG_{iwi} values correspond to more hydrophobic surfaces.

2.2.4. Attenuated Total Reflection – Fourier Transform Infrared Spectroscopy (ATR-FTIR)

ATR-FTIR was used to assess the chemical bonds present on the surface of cabbage leaves and biomimetic wax surfaces (Spectrum Two FT-IR Spectrometer with a UATR single bounce ATR accessory with a diamond internal reflection element and $LiTaO_3$ detector, PerkinElmer, UK). Background spectra were captured at room temperature before each measurement with no sample present to remove noise. For each sample, spectra were acquired over the range of 500 cm^{-1} to 4000 cm^{-1} using Spectrum IR software (PerkinElmer, UK), with each run made up of 4 scans and a resolution of 4 cm^{-1} (Saubade et al., 2021). Analysis was performed in triplicate and the results were expressed in absorbance using the average spectra.

2.3. Microbial adhesion to hydrocarbons (MATH) assay

Bacterial cell surface affinity to hydrocarbons was measured according to the MATH assay described by Whitehead et al. (2005). *E. coli* and *L. monocytogenes* overnight cultures were centrifuged at 567 *g* for 10 min, washed three times in PUM buffer pH 7.1 (PUM buffer: $K_2HPO_4.3H_2O$ 22.2, KH_2PO_4 7.26, urea 1.8, $MgSO_4.7H_2O$ 0.2 g/L) and resuspended to an optical density (OD) of 1.0 at 400 nm. A volume of 5 mL of washed cells suspended in PUM buffer was added to round bottom glass test tubes of 15 mm diameter and 1 mL n-hexadecane (Sigma-Aldrich, USA) was added to the test suspension. The suspensions were mixed by vortexing for 2 min and then incubated for 30 min at 37 °C. The lower aqueous phase was transferred to a cuvette and the OD was determined at 400 nm. The calculation used to determine the percentage affinity to hydrocarbons was (Eq. 1):

$$\%\ \ affinity = 1 - \frac{A}{A_0} \times 100 \quad [1]$$

where A_0 is the optical density of the microbial suspension measured at 400 nm before mixing, and A is the optical density following mixing with hydrocarbon and extraction of the aqueous phase measured at 400 nm.

2.4. Attachment, adhesion and retention assays

E. coli NCIB 9484, a common laboratory strain (Gill and Penney, 1977), or *L. monocytogenes* Scott A, an isolate from a foodborne outbreak (Briers et al., 2011), was inoculated into tryptone soy broth (TSB; Oxoid, UK) and incubated overnight at 37 °C with shaking (New Brunswick Scientific, USA). Appropriate dilutions in sterile distilled water were performed to obtain an OD of 0.5 at 540 nm, corresponding to 5.5×10^8 *E. coli* or *L. monocytogenes* colony forming units (CFU)/mL.

The biomimetic coupons and the fresh leaves were analysed for attachment (by spray plus wash), adhesion (by spray), and retention (by 1-h static incubation) assays with monocultures of the selected bacteria (McClements et al., 2021; Rajab et al., 2018). Before being used, the leaves were also cut into 15 mm diameter circles, washed with sterile distilled water and air-dried in a class 2 flow hood for 1 h. For attachment and adhesion assays, replicates of biomimetic surfaces and original leaves were attached to a vertical stainless steel tray and the bacterial suspension was sprayed (Spraycraft Universal Air Propellant, Shesto, UK) over the surfaces for 10 s. Immediately after spraying, the surfaces were divided into two sets (n = 3 each), one was laid horizontally and left to dry (adhesion assay) and the other was rinsed using a water spray bottle (attachment assay). For retention assays, surfaces were submerged

horizontally in 25 mL of cell suspension for 1 h at 37 °C (n = 3). Then, the cell suspension was poured off and the coupons or leaves were rinsed by dipping them in sterile distilled water. All surfaces from the three microbiological assays were then prepared for CFU enumeration by being added to 2 mL of phosphate-buffered saline (PBS; Oxoid, UK), vortexed for 1 min to ensure the removal of most adhered cells and plated out onto tryptone soy agar (TSA; Oxoid, UK). The agar plates were incubated for 18 h at 37 °C and the colony enumeration was performed in three independent experiments (n = 9). The surfaces were also prepared for SEM imaging (n = 1) (McClements et al., 2021).

2.5. *Statistical analysis*

Statistical analysis was carried out using non-parametric Mann-Whitney testing in SPSS® Statistics 26 software (IBM, USA). The error bars shown in the graphs correspond to the standard deviation (SD) or standard error (SE). Differences between samples were considered statistically significant for p values < 0.05.

3. Results and discussion

The leaves selected for replication in this study demonstrated slippery, superhydrophobic surfaces with sliding angles less than 10° such as have been described by the Cassie–Baxter model. In this model, the water droplet contacts the tips of the largest surface protrusions, resulting in a large air fraction which is trapped at the bottom of the surface, thus generating a non-wetting phenomenon, allowing water droplets to easily roll off the surfaces (Peng et al., 2013). The leaf surfaces were analysed for their surface properties, and the replicated surfaces were analysed in the same way

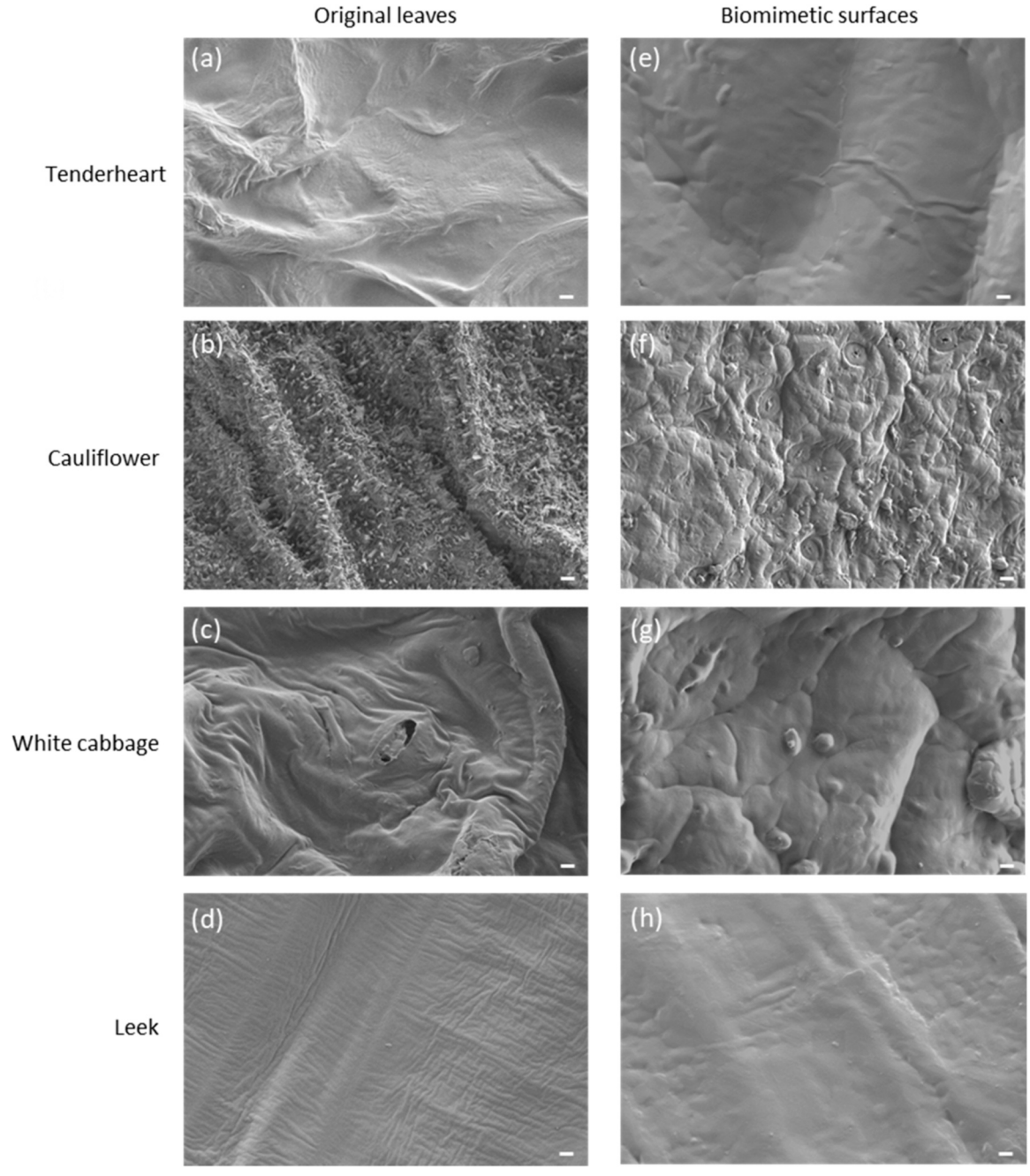

Fig. 1 – SEM micrographs of the (a-d) original leaves and (e-h) biomimetic wax surfaces of Tenderheart (a and e), Cauliflower (b and f), White cabbage (c and g), and Leek (d and h). Magnification of 5000 ×, Scale bar of 2 µm.

so that the degree of replication of the surfaces could be checked and to determine the effect of the surface properties on the attachment, adhesion and retention of *E. coli* and *L. monocytogenes*.

3.1. Surface characterization

SEM of the real and wax replica surfaces revealed that the macro-topographies of all the surfaces demonstrated some variations in roughness when compared to the original leaf surface (Fig. 1). The most obvious differences were seen between the original (Fig. 1b) and the replicated biomimetic Cauliflower leaf surfaces (Fig. 1f). Although the macro- and micro-topographies of the surfaces were well reproduced, the nano-topographies (< 0.5 µm and wax crystalline structures) on the biomimetic replicated surfaces were less evident. Legrand et al. (2021) demonstrated that the surface features of two bamboo varieties and *Ginkgo biloba* replicated using moulding methods and PDMS resulted in the loss of the nanometric features during the replication process. In addition, when the hierarchical patterns of water bamboo leaves (with features from the sub-millimeter to micron-scale range) were well reproduced, it was found that there was an absence of nanostructures on the replicated surface, and it was suggested that this was due to the melting of plant epidermal wax during the curing process (Guan et al., 2015).

Optical profilometry was used to quantify the surface roughness of the leaves using S_q as a qualitative comparator (Fig. 2) and S_{pv} (Fig. 3). The S_q value for the control wax surface (demonstrated by the black line in Fig. 2) was significantly lower than the S_q values of the biomimetic replica surfaces ($p < 0.05$). On the original leaf surfaces, the White cabbage demonstrated the lowest S_q value (3.5 µm), thus being the smoothest surface, whilst the roughest original leaf was the Leek (S_q = 5.4 µm). The least rough biomimetic replicated surface was the Leek (S_q = 2.0 µm), whereas the roughest biomimetic replicated surface was the White cabbage (S_q = 5.3 µm). There was only a significant difference demonstrated between the original and the biomimetic replicated surface for the Leek ($p < 0.05$). Thus, in agreement with the work by McClements et al. (2021), although the moulding techniques used were simpler than other production methodologies, there may be a loss in the resolution of the nano surface features. However, it has also been demonstrated that plants without the presence of macro- and micro-features can show superhydrophobicity (McClements et al., 2021). Hence, the relationship between the surface properties and the superhydrophobicity of a surface is still unclear.

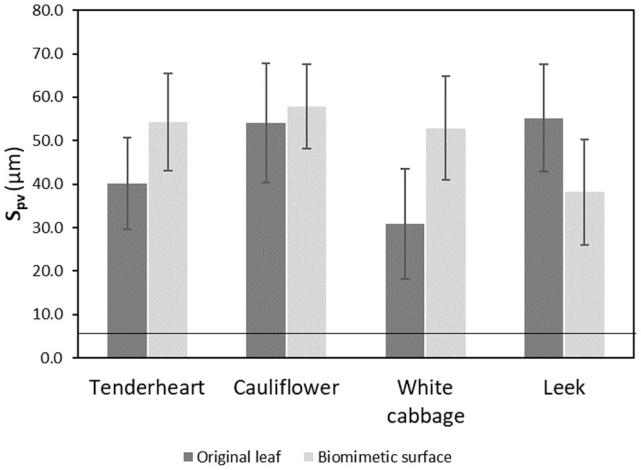

Fig. 3 – Peak to valley height (S_{pv}) values of the original leaf (Tenderheart, Cauliflower, White cabbage and Leek) and the corresponding biomimetic surface obtained by OP. The black line represents the value of the flat wax control.

The peak to valley height (S_{pv}) values were taken for the original leaves and the biomimetic replicas (Fig. 3). The S_{pv} value for the flat control wax surface (indicated by the black line) was significantly lower than the S_{pv} values of the biomimetic replica surfaces ($p < 0.05$). It was demonstrated that there was no significant difference in the values across the surfaces ($p > 0.05$), but this might be expected due to the

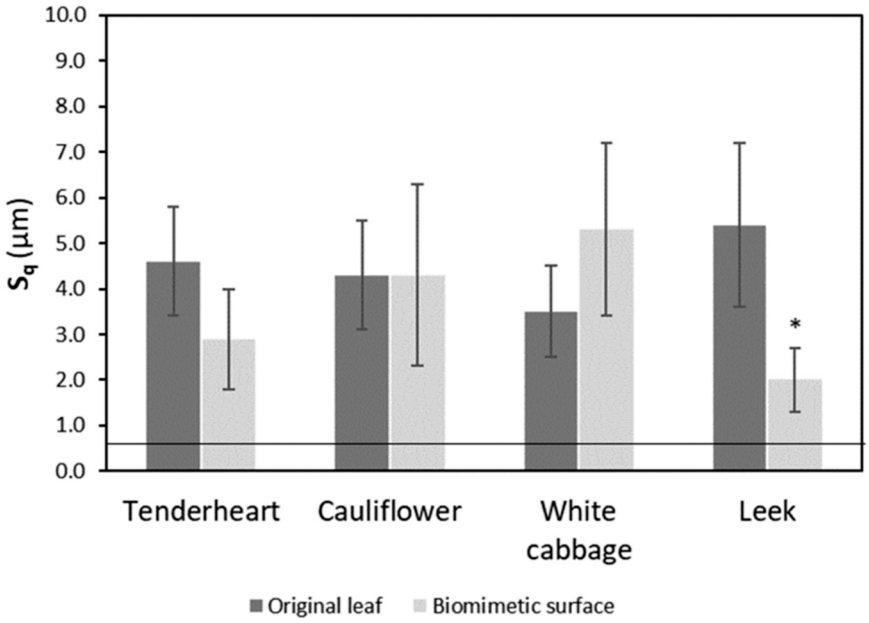

Fig. 2 – Root-mean-square roughness (S_q) of the original leaf (Tenderheart, Cauliflower, White cabbage and Leek) and the corresponding biomimetic surface obtained by OP. Values are means ± SEs. Asterisk denotes a significant difference between the original and replicates of the same leaf (* $p < 0.05$). The black line indicates the value of the flat wax control.

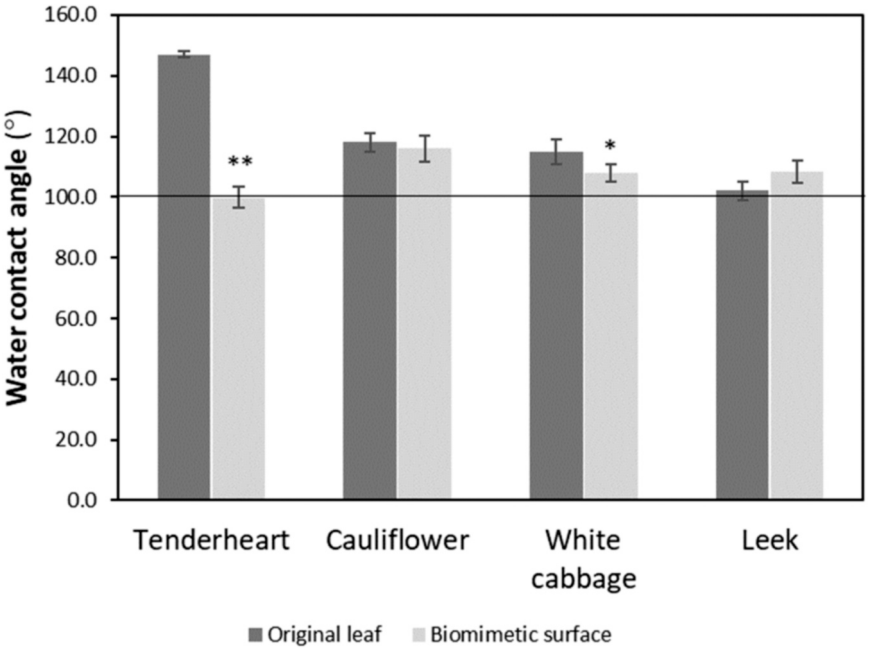

Fig. 4 – Water contact angles of the original leaf (Tenderheart, Cauliflower, White cabbage and Leek) and the corresponding biomimetic surface. Values are means ± SEs. Asterisks denote significant differences between the original and replicate of the same leaf (*$p < 0.05$ and **$p < 0.01$). The black line represents the value of the flat wax control.

variability in the surface topographies. Trends were observed, however, and for the natural surfaces, the Leek leaf demonstrated the greatest S_{pv} value (55.2 µm) and the White cabbage the lowest (30.9 µm), whilst on the biomimetic surfaces, the Cauliflower presented the greatest S_{pv} value (57.8 µm) and the Leek the lowest (38.2 µm).

Water contact angles were taken on the natural leaf and replicated biomimetic surfaces (Fig. 4). The results demonstrated that there were only significant differences between the natural and biomimetic surfaces for the Tenderheart ($p < 0.01$) and White cabbage ($p < 0.05$) leaves and replicas. There were no significant differences in the water contact angles between the leaves and replica surfaces for the Cauliflower and Leek. All the surfaces were hydrophobic (water contact angle > 90°), and even more hydrophobic following the addition of the biomimetic surface features to the flat control wax (100°).

The hydrophobicity (free energy of transfer, ΔG_{iwi}, Fig. 5) revealed that the White cabbage leaf had the most hydrophobic character (ΔG_{iwi} = −88.7 mJ/m^2), followed by Cauliflower, whilst Leek had the least hydrophobic surface tested (ΔG_{iwi} = −30.4 mJ/m^2). On the replica biomimetic surfaces, the

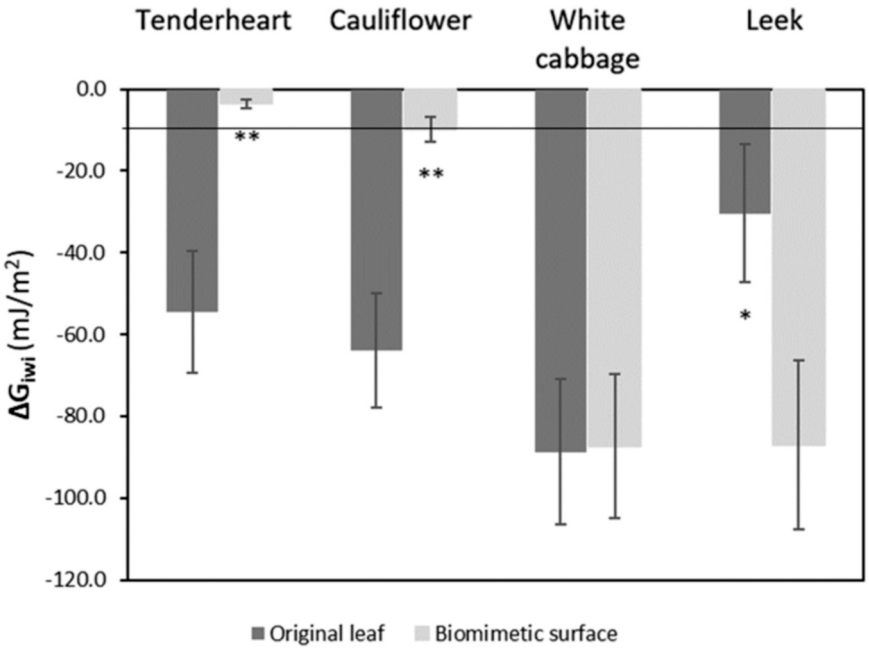

Fig. 5 – Hydrophobicity of the original leaf (Tenderheart, Cauliflower, White cabbage and Leek) and the corresponding biomimetic surface. Values are means ± SEs. Asterisks denote significant differences between the original and replicate of the same leaf (*$p < 0.05$ and **$p < 0.01$). The black line represents the value of the flat wax control.

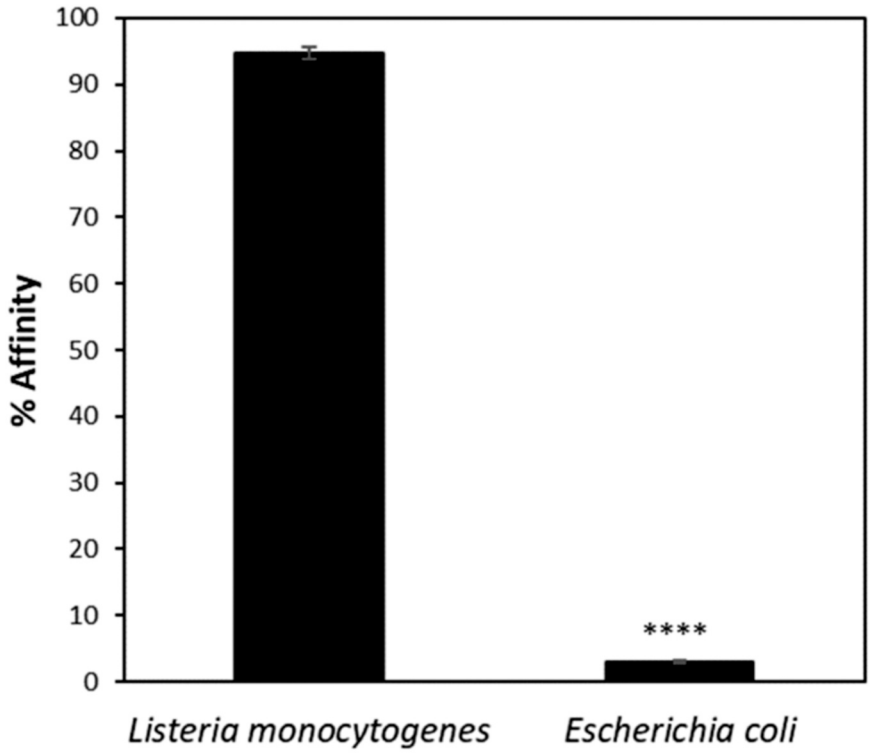

Fig. 6 – Percentage affinity of the bacterial strains *E. coli* and *L. monocytogenes* toward hydrocarbons. Values are means ± SDs. Symbol denotes significant difference between strains (** $p < 0.0001$).**

White cabbage was again the most hydrophobic (ΔG_{iwi} = –87.4 mJ/m^2), whilst the Tenderheart cabbage replica was the least hydrophobic surface (ΔG_{iwi} = –3.6 mJ/m^2). All the surfaces were more hydrophobic than the flat wax surface (indicated by the black line), except the Cauliflower (ΔG_{iwi} = –9.9 mJ/m^2) and the Tenderheart leaf replica (ΔG_{iwi} = –3.6 mJ/m^2).

The topography of a surface affects its wetting state (Timonen et al., 2013; Xu et al., 2013). It has been suggested that the attachment of water droplets is affected by surface roughness (Liu et al., 2022). Wenzel (1949) first explained the effect of surface roughness on contact angles whereby it was suggested that a solid substrate with a wetting tendency of less than 90° would wet more easily if its surface was rough. However, it was predicted that a solid substrate with a water-repelling tendency greater than 90° would repel water more if the surface was roughened (Wenzel, 1949). This theory was expanded by Cassie and Baxter (1944) to non-homogeneous and porous surfaces, and they stated that for a hydrophobic rough surface, the liquid repellency prevented the liquid from fully penetrating the depressions of the roughness morphology. When self-cleaning surfaces are considered, a low level of water drop adhesion to the surface is also important since a combination of high-water contact angle and low contact angle hysteresis is needed to decrease the force of the liquid drop adhesion, which enables the droplet to be able to set into motion (McHale et al., 2004; Richards et al., 2020). This may be one reason why the surface properties demonstrated inconsistencies between the original leaf and the biomimetic replicate surfaces. In agreement with our work, when replicated biomimetic surfaces were produced by Arango-Santander et al. (2021), it was found that in some cases, the natural leaves were highly hydrophobic, but such hydrophobicity could not be transferred to the metallic plates. In addition, it was found that the water contact angle values on artificial water bamboo leaf replicates were lower than on the original surfaces (Guan et al., 2015). This work is partially in agreement with our findings whereby two of our four replicated leaf surfaces, the Tenderheart and the White cabbage, also had significantly lower water contact angles than the original leaves ($p < 0.05$, Fig. 4). In another study, although the biomimetic wax surface and Gladioli leaves had extremely similar surface roughness parameters, the water contact angle of the Gladioli leaf was found to be significantly higher than the replicated biomimetic surface (McClements et al., 2021). Again, this is partially in agreement with the present study, where only the Tenderheart leaf had a significantly higher water contact angle (147°) than its biomimetic replica surface (99°) ($p < 0.01$). Hence, these studies demonstrated the challenges of using a simplified method to produce biomimetic surfaces.

The Microbial Adhesion To Hydrocarbon (MATH) assay was carried out to determine the hydrophobicity of the bacterial strains used in this study. It was found that *L. monocytogenes* was significantly more hydrophobic (95 %) than *E. coli* (3 %) (Fig. 6). In agreement with these results, *E. coli* has been reported as being hydrophilic in nature (Rivas et al., 2005), although the hydrophobicity of *L. monocytogenes* can vary depending on a number of factors (Lee et al., 2017). These may include the hydrocarbon droplets contributing to the absorbance values during spectrophotometric measurements (Zoueki et al., 2010), and factors such as the buffer, ionic strength, pH, temperature, duration of phase separation, mixing time, ratio of organic to liquid phase, and turbidity of the initial cell suspension (Nachtigall et al., 2019).

3.2. *Attachment, adhesion and retention assays*

In general, *L. monocytogenes* (Gram-positive bacteria) bound to both the original leaf and biomimetic replicated surfaces in

lower numbers than the Gram-negative bacteria *E. coli* (Figs. 7 to 9). This was most evident in attachment and retention assays where a difference of ~ 0.30 Log CFU/cm^2 existed between species, regardless of the surface type. This could be related to the surface hydrophobicity of the *L. monocytogenes* strain whereby it was found to be significantly more hydrophobic than *E. coli* (Fig. 6). This is in contrast to the work by McClements et al. (2021) who found that only following retention assays that *L. monocytogenes* bound in lower numbers to Gladioli leaf (3.83×10^3 CFU/cm^2) and biomimetic replica surfaces (6.94×10^1 CFU/cm^2). Further, in previous work on smoother surfaces, it was demonstrated that *L. monocytogenes* and *Staphylococcus aureus* retention to the surfaces were mostly affected by surface microtopography, whereas retention of *E. coli* to the coatings was mostly affected by the coating physicochemistry (Whitehead et al., 2015), and this may be a clear effect of topography. Although there is conflicting evidence, it has been suggested that the hydrophobicity of a bacterial cell is largely influenced by the different chemistries of the surface of the cell (van der Mei et al., 1991). Positive relationships between physicochemical surface properties and bacterial attachment have been reported (Liu et al., 2004), however, others have found no evidence of such relationships (Bettelheim et al., 1995; Rivas et al., 2007).

Following the attachment assays, from the results of the original leaves, the Tenderheart cabbage (which were the least hydrophobic) attached most *E. coli* and *L. monocytogenes* (6.85 Log CFU/cm^2 and 6.54 Log CFU/cm^2, respectively; Fig. 7a and b). However, *L. monocytogenes* cells were also attached to the Leek surfaces in similar numbers (6.53 Log CFU/cm^2), which was the roughest surface and the second most hydrophobic leaf surface. *E. coli* were least attached on the Leek leaves (6.52 log CFU/cm^2), which were the roughest surfaces with the second greatest hydrophobicity. On the other hand, *L. monocytogenes* were least attached to the White cabbage surface (5.68 Log CFU/cm^2), which was the smoothest and most hydrophobic surface. Interestingly, the *E. coli* attachment to the natural leaf surfaces followed the same pattern as the water contact angle of the surfaces, whereby a decrease in water contact angle resulted in a decrease in the number of *E. coli* attached.

On the biomimetic replicate surfaces, *E. coli* was attached in the greatest numbers on the replica biomimetic Leek surface (6.40 Log CFU/cm^2) (smoothest and least hydrophobic), and in the least numbers on the White cabbage biomimetic surface (5.49 Log CFU/cm^2) (roughest and most hydrophobic). *L. monocytogenes* was attached in the greatest numbers on the Leek biomimetic surface (6.44 Log CFU/cm^2) (smoothest and least hydrophobic), and in the least numbers on the White cabbage biomimetic surface (6.02 Log CFU/cm^2) (roughest and most hydrophobic). Hence, for *E. coli*, cell attachment on both the leaves and biomimetic replicate surfaces, and *L. monocytogenes* on the biomimetic replicate surfaces, was influenced by both surface hydrophobicity and roughness (i.e., lowest cell numbers on least hydrophobic, smooth surfaces). However, on the leaf surfaces, *L. monocytogenes* was most influenced by the surface roughness. There was no relationship between the S_{pv}values and the attachment of the bacteria on the natural leaf or biomimetic replicated surfaces. The attachment of the bacteria to the natural and biomimetic surfaces was significantly different when compared to the flat wax control surface with the exception of *E. coli* on the White cabbage surface, suggesting

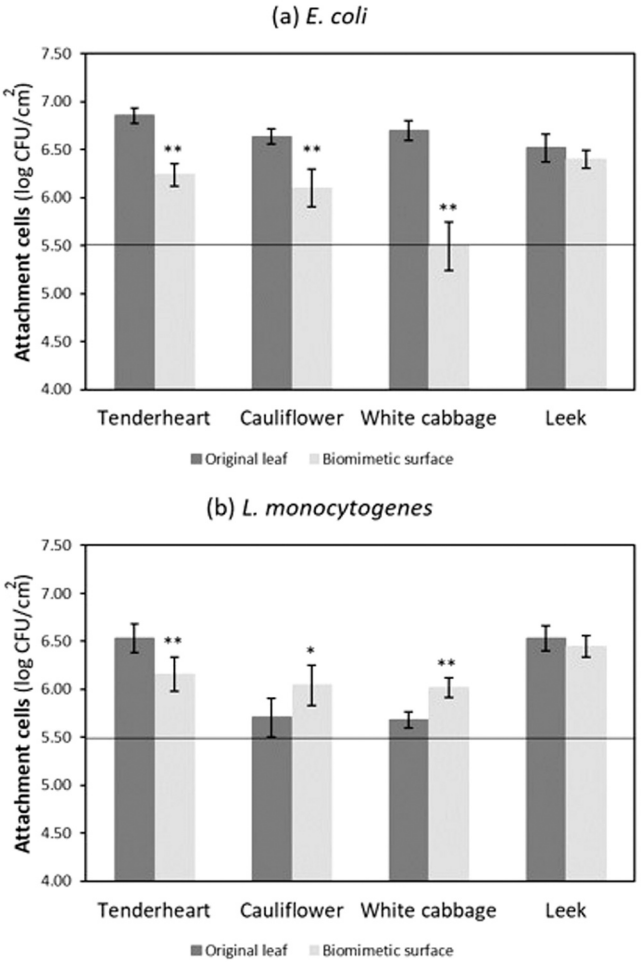

Fig. 7 – Number of (a) *E. coli* and (b) *L. monocytogenes* culturable cells following the attachment assay on the original leaf (Tenderheart, Cauliflower, White cabbage and Leek) and the corresponding biomimetic surface. The means ± SDs for three independent experiments are presented. Asterisks denote significant differences between the original and replicate of the same leaf (*$p < 0.05$ and **$p < 0.01$). The black lines indicate the values of the flat wax control.

that in situations whereby no rinsing is involved, such surfaces would not be suitable for reducing bacterial attachment to surfaces.

For the adhesion assays (Fig. 8), *E. coli* and *L. monocytogenes* adhered on the leaf surfaces in the greatest numbers to the Tenderheart cabbage (7.00 Log CFU/cm^2) and Cauliflower leaves (6.56 Log CFU/cm^2). *E. coli* and *L. monocytogenes* adhered on the leaf surfaces in the lowest numbers to the White cabbage (6.50 Log CFU/cm^2 and 5.51 Log CFU/cm^2, respectively). For the adhesion assays on the biomimetic surfaces, *E. coli* (Fig. 8a) and *L. monocytogenes* (Fig. 8b) adhered on the surfaces in the greatest numbers to the biomimetic Leek (6.61 Log CFU/cm^2) and the White cabbage surfaces (6.78 Log CFU/cm^2). Both bacterial strains adhered on the biomimetic surfaces in the lowest numbers to the Tenderheart cabbage (6.27 Log CFU/cm^2) and the Cauliflower surfaces (6.12 Log CFU/cm^2). In summary, following the use of the adhesion assay, it was difficult to elucidate the surface properties that reduced microbial adhesion. However, it could be speculated that the use of surfaces with a S_q value between 2.9 and 4.3 µm, and a ΔG_{iwi} value between - 54.5 and - 63.9 mJ/m^2 resulted in the

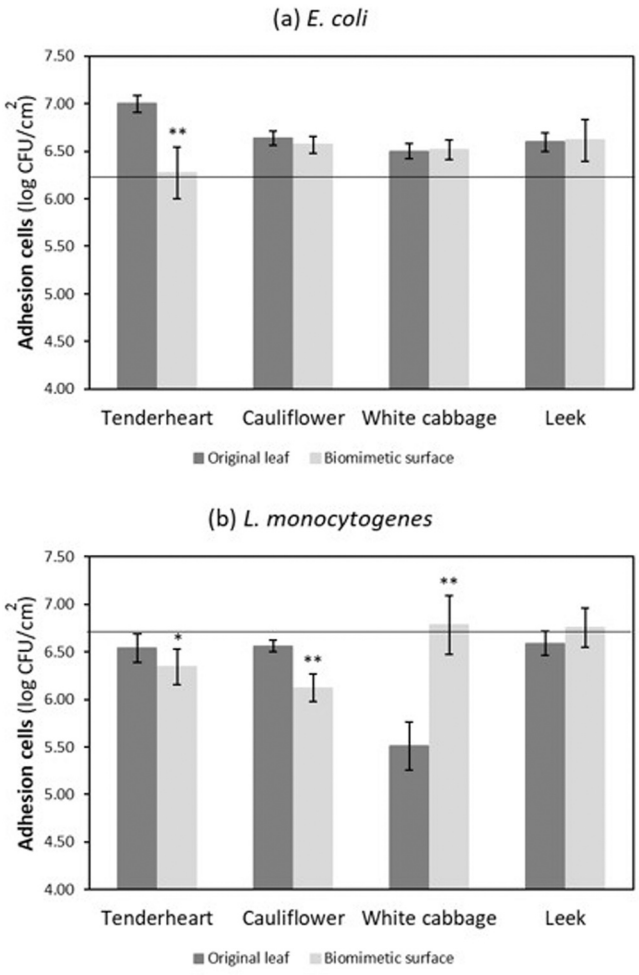

Fig. 8 – Number of (a) *E. coli* and (b) *L. monocytogenes* culturable cells following the adhesion assay on the original leaf and the corresponding biomimetic surface. The means ± SDs for three independent experiments are presented. Asterisks denote significant differences between the original and replicate of the same leaf (*$p < 0.05$ and **$p < 0.01$). The black lines indicate the values of the flat wax control.

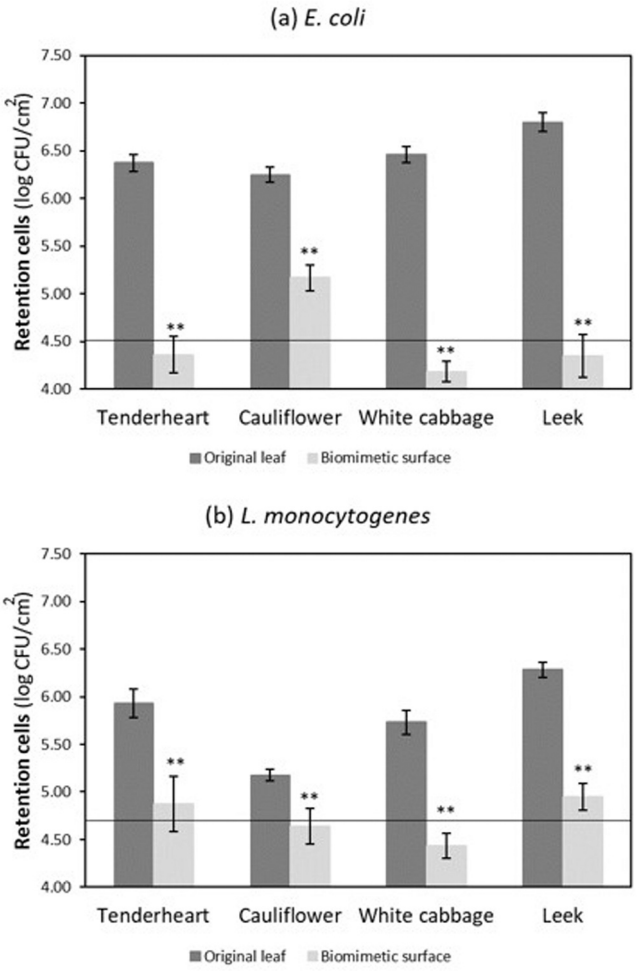

Fig. 9 – Number of (a) *E. coli* and (b) *L. monocytogenes* culturable cells following the retention assay on the original leaf and the corresponding biomimetic surface. The means ± SDs for three independent experiments are presented. Asterisks denote significant differences between the original and replicate of the same leaf (*$p < 0.05$ and **$p < 0.01$). The black lines indicate the values of the flat wax control.

least bacterial adhesion on the surfaces. There was no relationship between the S_{pv} values or the water contact angles and the adhesion of bacteria on the natural leaf or biomimetic replicated surfaces.

For the adhesion assays using *E. coli*, it can be suggested that these surfaces would not be suitable for use in a system whereby bacteria become attached and then are rinsed from surfaces since the bacteria were adhered in greater numbers than the control, with the exception of *E. coli* on the biomimetic Tenderheart surface. However, when using *L. monocytogenes*, it was demonstrated that all natural leaves and the Tenderheart and Cauliflower biomimetic replicated leaves resulted in significantly lowered adhesion of cells when compared to the control surface.

For the retention assays on the original leaf surfaces, *E. coli* (Fig. 9a) and *L. monocytogenes* (Fig. 9b) were retained in the greatest numbers to the Leek leaf surface (6.80 Log CFU/cm^2 and 6.28 Log CFU/cm^2, respectively). Nevertheless, *E. coli* and *L. monocytogenes* retained in the lowest numbers to the Cauliflower leaf (6.25 Log CFU/cm^2 and 5.18 Log CFU/cm^2, respectively). Following retention assays on the biomimetic surfaces, *E. coli* and *L. monocytogenes* were retained in the greatest numbers to the Cauliflower (5.17 Log CFU/cm^2) and Leek (4.95 Log CFU/cm^2), and in the lowest numbers to the White cabbage replicate surface (4.18 Log CFU/cm^2 and 4.44 Log CFU/cm^2, respectively). The retention of *E. coli* to the natural leaf surfaces was influenced by the water contact angle of the biomimetic replicated surfaces since a lower water contact angle resulted in a lower amount of adhered *E. coli* retained onto the surface. Therefore, on the plant leaves, the rough, hydrophobic surfaces increased the retention of bacterial cells, whilst surfaces with S_q values around 4.3 µm and which were least hydrophobic reduced bacterial retention. On the replicated biomimetic surfaces, the rougher, hydrophobic surfaces decreased bacterial retention. When using *E. coli*, the replicated biomimetic surfaces for the Tenderheart, White cabbage and Leek, and for *L. monocytogenes*, the White cabbage and Cauliflower demonstrated lower numbers of retained bacteria than the control surfaces (with statistical significance only for the White cabbage, $p < 0.05$).

FTIR was carried out to determine the chemical bonds on the natural leaves and the replicated biomimetic surfaces

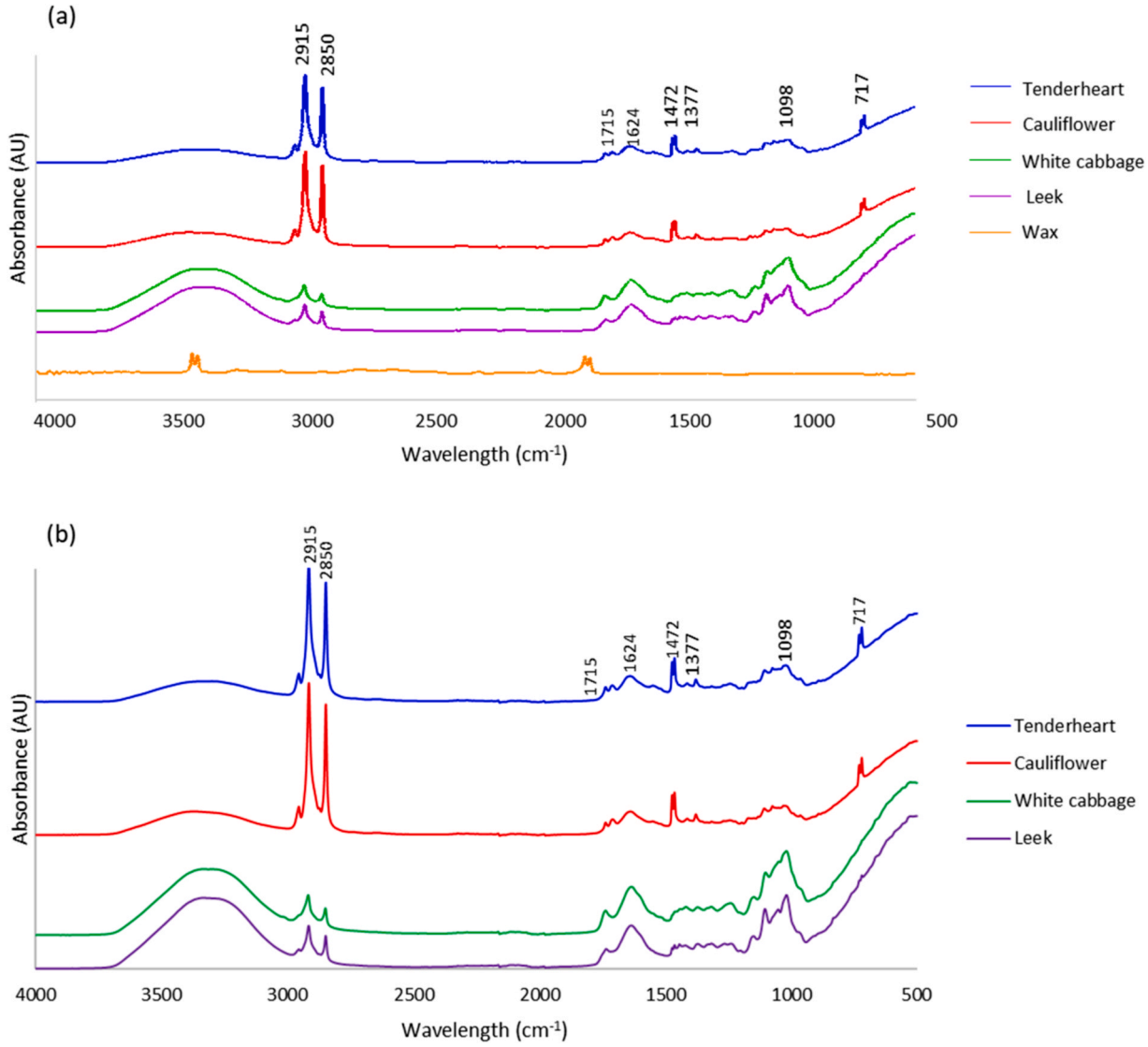

Fig. 10 – FTIR spectra of (a) original leaves and wax, and (b) biomimetic wax surfaces.

(Fig. 10). It was demonstrated that on the natural leaves (Fig. 10a) and biomimetic surfaces (Fig. 10b) similar peaks were obtained, suggesting the transfer of chemical species from the leaves onto the biomimetic replicated surfaces. A C-H stretch was detected at 2915 cm^{-1}, whilst at 2850 cm^{-1} a symmetrical νs CH_2 methylene stretching band was demonstrated. The peak at 1715 cm^{-1} was indicative of carbonyl (C═O) ester-based compounds, whilst the peak at 1624 cm^{-1} may have been H–O bending modes of residual water molecule. A C–H bend or scissoring was seen at 1472 cm^{-1}, and at 1377 cm^{-1} a peak indicative of δ CH_3 aliphatic chains of fatty acids was observed (Oleszko et al., 2015; Rohman et al., 2011; Sánchez-Alonso et al., 2012). At 1098 cm^{-1}, carboxyl symmetrical stretching vibrations were demonstrated and at 717 cm^{-1}, C-H rocking (ρ CH_2) bands in long-chain alkanes were detected (McClements et al., 2021). On the flat wax surfaces, peaks observed at 3300 cm^{-1} were indicative of O-H stretching from residual water and the peak at 1850 cm^{-1} demonstrated C-H bending.

The SEM images of the natural leaves and biomimetic surfaces with attached, adhered and retained bacteria were analysed (Fig. 11). It could be observed on the natural surfaces for *E. coli* (Fig. 11a-c) and *L. monocytogenes* (Fig. 11g-i) that bacteria were bound to the surface, particularly in the surface topography features. However, this pattern was less evident on the biomimetic replicated surfaces for both types of bacteria (*E. coli* in Fig. 11d-f and *L. monocytogenes* in Fig. 11j-l).

When comparing biomimetic with the original leaf surface, it was observed that, in most cases, all types of replica biomimetic surfaces were more efficient at reducing the numbers of bacteria that bound to the surface than the natural leaves. These higher reduction rates were particularly noticeable in the attachment assays with *E. coli* (Fig. 7a), where the biomimetic surfaces showed on average less 0.62 Log CFU/cm^2, as well as in the bacterial retention assays with both bacteria (Fig. 9a and b). In this case, reductions of on average 1.92 and 1.05 Log CFU/cm^2 were achieved for *E. coli* and *L. monocytogenes* ($p < 0.01$), respectively, with biomimetic surfaces of White cabbage and Leek showing to be the most promising surfaces. This is in agreement with the work by McClements et al. (2021) who compared the self-cleaning properties of biomimetic-produced surfaces against *E. coli* and *L. monocytogenes*, where it was found that the biomimetic surfaces retained fewer bacteria than the control surfaces.

In general, for the attachment assays, the lowest cell numbers occurred on the least hydrophobic, smooth surfaces. Following the adhesion assays, the use of surfaces

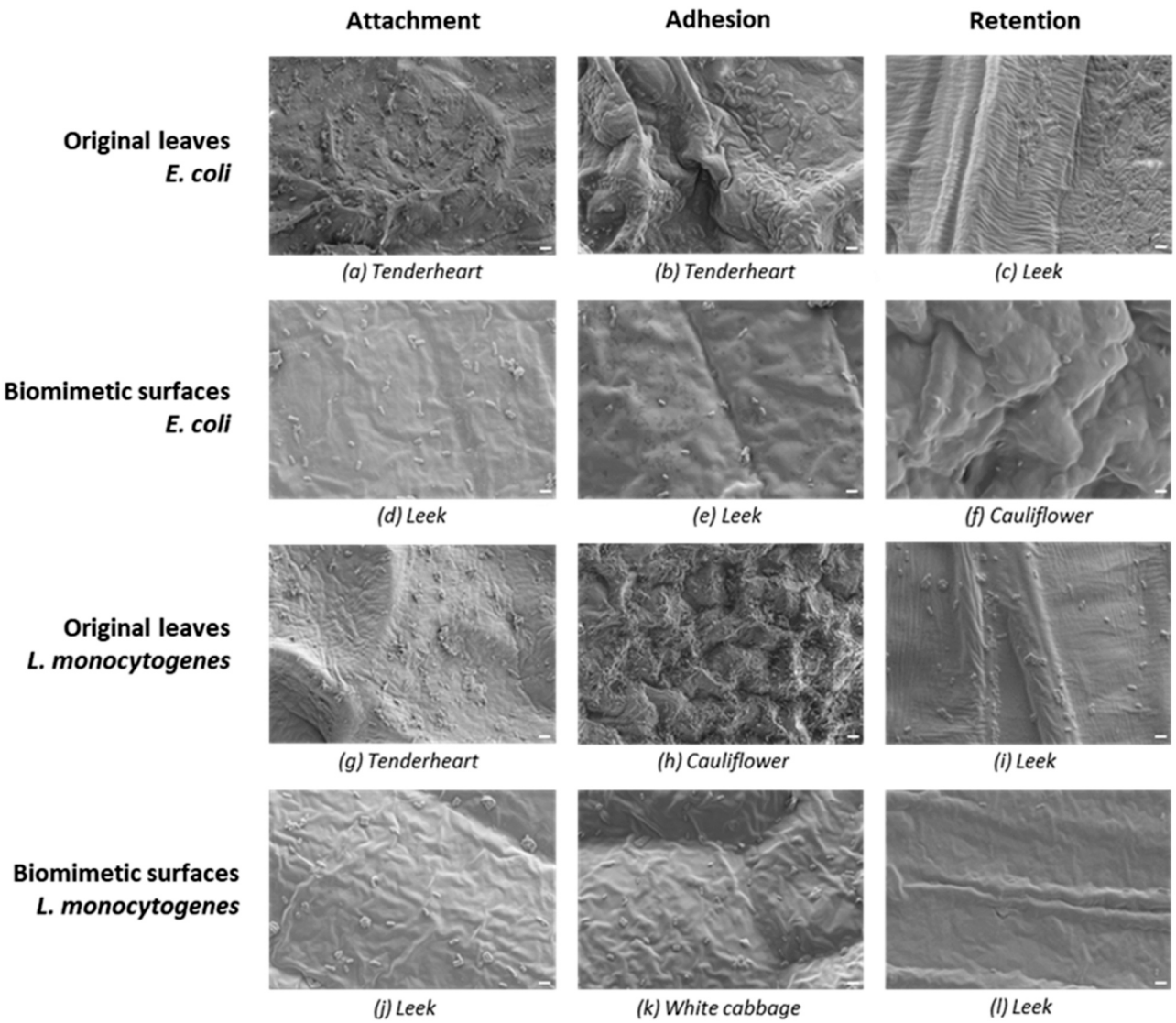

Fig. 11 – SEM images of the (a-c, g-i) original leaves and (d-f, j-l) biomimetic wax surfaces that attached, adhered, or retained the greatest numbers of bacteria. Magnification of 5000 ×, Scale bar of 2 µm.

with an intermediate S_q and ΔG_{iwi} demonstrated the lowest bacterial adhesion. However, following the retention assays, it seems that the chemistry of the surface may have affected the results since opposite surface effects were demonstrated to reduce cell retention on the leaf which was the least hydrophobic and on the biomimetic surfaces which were rougher and hydrophobic. This is an interesting concept since it is generally believed that rougher surfaces increase bacterial retention. However, it has been shown that this phenomenon is an interplay of the relationship between the size and shape of the bacteria, alongside the size and shape of the surface features (Verran et al., 2010). In addition, the Cassie-Baxter effect may also impede the effect of surface topography on bacterial retention since a high-water contact angle and low-contact angle hysteresis will enable a droplet to sit on top of the surface features (Cansoy et al., 2011). As demonstrated by the surface topographies, biomimetic surfaces are complex, certainly in terms of their topographies. If the surface features are of certain dimensions, or the surface becomes compromised so that the Cassie-Baxter phenomenon no longer applies, then there is the possibility that the surface roughness will trap the bacterial cells. This is a phenomenon that requires further investigation.

In agreement with Liauw et al. (2020), the overall results suggest that the different methods exerted different influences on the surface and bacterial binding. This is an important finding since this may be one of the reasons for the conflicting evidence regarding the effect of surface properties on bacterial binding. The attachment assays include a spraying step directly following cell application to the surface, and hence the bacteria only have a few seconds to bind. In this case, the surfaces that were the least hydrophobic and smooth had the least bacteria, suggesting that the immediate inclusion of a washing step altered the hydration dynamics between the surface and bacteria. Such an assay may be representative of where unwanted fouling occurs on a surface and is immediately removed. The adhesion assay does not involve a wash step, so the bacteria that bind to the surface are able to adhere, and in this case, surfaces with intermediate S_q and ΔG_{iwi} demonstrated the least bacterial retention. Such a scenario may occur when fouling arises on a surface but is not immediately cleaned. In the retention assay, the bacteria could bind to the surface whilst in suspension for a longer time, showing different interactions that can only be assumed to be due in part to the chemistry of the surface, but this requires further investigation. Such an assay

may be representative of foodstuffs that are stored in a vat for a longer period of time. In agreement with our work, bacterial binding on replicated biomimetic surfaces is not a straightforward phenomenon. Biomimetic surfaces that were prepared using the soft lithography technique demonstrated that two of the surface models used showed positive results for reduction of *C. aurea* and *C. esculenta*, while the other showed an increase in bacterial adhesion (*S. molesta*) (Arango-Santander et al., 2021). However, other authors have demonstrated that biomimetic surfaces inhibited *E. coli* adhesion (Hu et al., 2018) and have a bacteriostatic effect on *S. aureus* (Li et al., 2013). On reproduced *Laminaria japonica* biomimetic surfaces, the antifouling effect against *E. coli* was also found to be effective (Zhao et al., 2020). Hence, the findings from this work show that, in addition to surface attributes such as hydrophobicity and roughness, the biological factors and environment, as well as the type of methodologies used, need to be taken into consideration when designing self-cleaning surfaces based on biomimetic principles, particularly if the surface is to be used in future scale up.

4. Conclusions

The replication of biological surfaces has great potential in applied surface technology. These preliminary results showed that via a casting approach, wax surfaces mimicking the structure of vegetable leaves could be prepared and that these surfaces seem to be promising in preventing bacterial binding. In general, for the attachment assays, the lowest cell numbers occurred on the least hydrophobic and smooth surfaces, regardless of the strain. For the adhesion assays, using *L. monocytogenes*, the Tenderheart and Cauliflower biomimetic leaves resulted in lowered cell adhesion. Following the retention assays, the White cabbage demonstrated lower cell retention for both types of bacteria on the biomimetic surface compared to the flat control surface. In further experiments, we will concentrate on the choice of appropriate multispecies cultures and polymers to get closer to the conditions found in real scenarios where biofilms are established in the food industry.

Funding

This work was financially supported by: LA/P/0045/2020 (ALiCE), UIDB/00511/2020 and UIDP/00511/2020 (LEPABE), funded by national funds through FCT/MCTES (PIDDAC); the European Union's Horizon 2020 Research and Innovation Programme under grant agreement no. 952471 (SurfSAFE). L.C.G. thanks the Portuguese Foundation for Science and Technology (FCT) for the financial support through the Scientific Employment Stimulus - Individual Call - [CEECIND/01700/2017]. All authors thank also Manchester Metropolitan University for the financial support of this work.

Declaration of Competing Interest

The authors have no competing or conflicts of interest.

References

Alon, H., Vitoshkin, H., Ziv, C., Gunamalai, L., Sinitsa, S., Kleiman, M., 2022. Self-cleaning biomimetic surfaces: the effect of microstructure and hydrophobicity on conidia repellence. Materials 15, 2526. https://doi.org/10.3390/ma15072526

Arango-Santander, S., Serna, L., Sanchez-Garzon, J., Franco, J., 2021. Evaluation of *Streptococcus mutans* adhesion to stainless steel surfaces modified using different topographies following a biomimetic approach. Coatings 11, 829. https://doi.org/10.3390/coatings11070829

Arreguin-Campos, R., Eersels, K., Lowdon, J.W., Rogosic, R., Heidt, B., Caldara, M., Jiménez-Monroy, K.L., Diliën, H., Cleij, T.J., van Grinsven, B., 2021. Biomimetic sensing of *Escherichia coli* at the solid-liquid interface: From surface-imprinted polymer synthesis toward real sample sensing in food safety. Microchem J. 169, 106554. https://doi.org/10.1016/j.microc.2021.106554

Bettelheim, K.A., Chang, B.J., Elliott, S.J., Gunzburg, S.T., Pearce, J.L., 1995. Virulence factors associated with strains of *Escherichia coli* from cases of sudden infant death syndrome (SIDS). Comp. Immunol. Microbiol. Infect. Dis. 18, 179–188. https://doi.org/10.1016/0147-9571(94)00026-Q

Briers, Y., Klumpp, J., Schuppler, M., Loessner, M.J., 2011. Genome sequence of *Listeria monocytogenes* Scott A, a clinical isolate from a food-borne listeriosis outbreak. J. Bacteriol. 193, 4284–4285. https://doi.org/10.1128/JB.05328-11

Cansoy, C.E., Erbil, H.Y., Akar, O., Akin, T., 2011. Effect of pattern size and geometry on the use of Cassie–Baxter equation for superhydrophobic surfaces. Colloids Surf. A Physicochem. Eng. Asp. 386, 116–124. https://doi.org/10.1016/j.colsurfa.2011.07.005

Cassie, A.B.D., Baxter, S., 1944. Wettability of porous surfaces. J. Chem. Soc. Faraday Trans. 40, 546–551. https://doi.org/10.1039/TF9444000546

Chen, L., Duan, Y., Cui, M., Huang, R., Su, R., Qi, W., He, Z., 2021. Biomimetic surface coatings for marine antifouling: Natural antifoulants, synthetic polymers and surface microtopography. Sci. Total Environ. 766, 144469. https://doi.org/10.1016/j.scitotenv.2020.144469

Chmielewski, R.A.N., Frank, J.F., 2003. Biofilm formation and control in food processing facilities. Compr. Rev. Food Sci. Food Saf. 2, 22–32. https://doi.org/10.1111/j.1541-4337.2003.tb00012.x

Damodaran, V.B., Murthy, N.S., 2016. Bio-inspired strategies for designing antifouling biomaterials. Biomater. Res. 20, 18. https://doi.org/10.1186/s40824-016-0064-4

de Grandi, A.Z., Pinto, U.M., Destro, M.T., 2018. Dual-species biofilm of *Listeria monocytogenes* and *Escherichia coli* on stainless steel surface. World J. Microbiol. Biotechnol. 34, 61. https://doi.org/10.1007/s11274-018-2445-4

Gill, C.O., Penney, N., 1977. Penetration of bacteria into meat. Appl. Environ. Microbiol. 33, 1284–1286. https://doi.org/10.1128/aem.33.6.1284-1286.1977

Guan, H., Han, Z., Cao, H., Niu, S., Qian, Z., Ye, J., Ren, L., 2015. Characterization of multi-scale morphology and superhydrophobicity of water bamboo leaves and biomimetic polydimethylsiloxane (PDMS) replicas. J. Bionic Eng. 12, 624–633. https://doi.org/10.1016/S1672-6529(14)60152-9

Hu, L., Zhang, L., Wang, D., Lin, X., Chen, Y., 2018. Fabrication of biomimetic superhydrophobic surface based on nanosecond laser-treated titanium alloy surface and organic polysilazane composite coating. Colloids Surf. A: Physicochem. Eng. Asp. 555, 515–524. https://doi.org/10.1016/j.colsurfa.2018.07.029

Huffman, B., Mazrouei, R., Bevelheimer, J., Shavezipur, M., 2017. Three-Dimensional Biomimetic Biosensors for Food Safety Applications, ASME 2017 International Design Engineering Technical Conferences and Computers and Information in Engineering Conference.

Klayman, B.J., Volden, P.A., Stewart, P.S., Camper, A.K., 2009. *Escherichia coli* O157:H7 requires colonizing partner to adhere and persist in a capillary flow cell. Environ. Sci. Technol. 43, 2105–2111. https://doi.org/10.1021/es802218q

Lazzini, G., Romoli, L., Blunt, L., Gemini, L., 2017. Design and characterization of textured surfaces for applications in the food industry. Surf. Topogr. 5, 044005. https://doi.org/10.1088/2051-672X/aa939f

Lee, B.-H., Hébraud, M., Bernardi, T., 2017. Increased adhesion of *Listeria monocytogenes* strains to abiotic surfaces under cold stress. Front. Microbiol. 8. https://doi.org/10.3389/fmicb.2017.02221

Legrand, Q., Benayoun, S., Valette, S., 2021. Biomimetic approach for the elaboration of highly hydrophobic surfaces: study of the links between morphology and wettability. Biomimetics 6, 38. https://doi.org/10.3390/biomimetics6020038

Li, J., Liu, X., Qiao, Y., Zhu, H., Li, J., Cui, T., Ding, C., 2013. Enhanced bioactivity and bacteriostasis effect of TiO_2 nanofilms with favorable biomimetic architectures on titanium surface. RSC Adv. 3, 11214–11225. https://doi.org/10.1039/C3RA23252B

Liauw, C.M., Slate, A.J., Butler, J.A., Wilson-Nieuwenhuis, J.S.T., Deisenroth, T., Preuss, A., Verran, J., Whitehead, K.A., 2020. The effect of surface hydrophobicity on the attachment of fungal conidia to substrates of polyvinyl acetate and polyvinyl alcohol. J. Polym. Environ. 28, 1450–1464. https://doi.org/10.1007/s10924-020-01693-z

Liu, Y., Yang, S.F., Li, Y., Xu, H., Qin, L., Tay, J.H., 2004. The influence of cell and substratum surface hydrophobicities on microbial attachment. J. Biotechnol. 110, 251–256. https://doi.org/10.1016/j.jbiotec.2004.02.012

Liu, Z., Niu, T., Lei, Y., Luo, Y., 2022. Metal surface wettability modification by nanosecond laser surface texturing: a review. Biosurf. Biotribol. 8, 95–120. https://doi.org/10.1049/bsb2.12039

Matinha-Cardoso, J., Mota, R., Gomes, L.C., Gomes, M., Mergulhão, F.J., Tamagnini, P., Martins, M.C.L., Costa, F., 2021. Surface activation of medical grade polyurethane for the covalent immobilization of an anti-adhesive biopolymeric coating. J. Mater. Chem. B 9, 3705–3715. https://doi.org/10.1039/D1TB00278C

McClements, J., Gomes, L.C., Spall, J., Saubade, F., Akhidime, D., Peeters, M., Mergulhão, F.J., Whitehead, K.A., 2021. Celebrating the centenary in polymer science: Drawing inspiration from nature to develop anti-fouling coatings. The development of biomimetic polymer surfaces and their effect on bacterial fouling. Pure Appl. Chem. https://doi.org/10.1515/pac-2021-0108

McHale, G., Shirtcliffe, N.J., Newton, M.I., 2004. Super-hydrophobic and super-wetting surfaces: analytical potential. Analyst 129, 284–287. https://doi.org/10.1039/B400567H

Moerman, F., 2014. Antimicrobial materials, coatings and biomimetic surfaces with modified microtography to control microbial fouling of product contact surfaces within food processing equipment: legislation, requirements, effectiveness and challenges. J. Hyg. Eng. Des. 7, 8–29.

Monteiro, N.O., Oliveira, C., Silva, T.H., Martins, A., Fangueiro, J.F., Reis, R.L., Neves, N.M., 2022. Biomimetic surface topography from the *Rubus fruticosus* leaf as a guidance of angiogenesis in tissue engineering applications. ACS Biomater. Sci. Eng. 8, 2943–2953. https://doi.org/10.1021/acsbiomaterials.2c00264

Moreira, J.M.R., Fulgêncio, R., Oliveira, F., Machado, I., Bialuch, I., Melo, L.F., Simões, M., Mergulhão, F.J., 2016. Evaluation of SICON® surfaces for biofouling mitigation in critical process areas. Food Bioprod. Process. 98, 173–180. https://doi.org/10.1016/j.fbp.2016.01.009

Nachtigall, C., Weber, C., Rothenburger, S., Jaros, D., Rohm, H., 2019. Test parameters and cell chain length of *Streptococcus thermophilus* affect the microbial adhesion to hydrocarbons assay: a methodical approach. FEMS Microbiol. Lett. 366. https://doi.org/10.1093/femsle/fnz150

Oleszko, A., Olsztyńska-Janus, S., Walski, T., Grzeszczuk-Kuć, K., Bujok, J., Gałecka, K., Czerski, A., Witkiewicz, W., Komorowska, M., 2015. Application of FTIR-ATR Spectroscopy to determine the extent of lipid peroxidation in plasma during haemodialysis. BioMed. Res. Int. 2015, 245607. https://doi.org/10.1155/2015/245607

Peng, S., Tian, D., Miao, X., Yang, X., Deng, W., 2013. Designing robust alumina nanowires-on-nanopores structures: superhydrophobic surfaces with slippery or sticky water adhesion. J. Colloid Interface Sci. 409, 18–24. https://doi.org/10.1016/j.jcis.2013.07.059

Rajab, F.H., Liauw, C.M., Benson, P.S., Li, L., Whitehead, K.A., 2017. Production of hybrid macro/micro/nano surface structures on Ti_6Al_4V surfaces by picosecond laser surface texturing and their antifouling characteristics. Colloids Surf. B: Biointerfaces 160, 688–696. https://doi.org/10.1016/j.colsurfb.2017.10.008

Rajab, F.H., Liauw, C.M., Benson, P.S., Li, L., Whitehead, K.A., 2018. Picosecond laser treatment production of hierarchical structured stainless steel to reduce bacterial fouling. Food Bioprod. Process. 109, 29–40. https://doi.org/10.1016/j.fbp.2018.02.009

Ramachandran, R., Sobolev, K., Nosonovsky, M., 2015. Dynamics of droplet impact on hydrophobic/icephobic concrete with the potential for superhydrophobicity. Langmuir 31, 1437–1444. https://doi.org/10.1021/la504626f

Richards, C., Slaimi, A., O'Connor, N.E., Barrett, A., Kwiatkowska, S., Regan, F., 2020. Bio-inspired surface texture modification as a viable feature of future aquatic antifouling strategies: a review. Int. J. Mol. Sci. 21. https://doi.org/10.3390/ijms21145063

Rivas, L., Fegan, N., Dykes, G.A., 2005. Physicochemical properties of Shiga toxigenic *Escherichia coli*. J. Appl. Microbiol. 99, 716–727. https://doi.org/10.1111/j.1365-2672.2005.02688.x

Rivas, L., Fegan, N., Dykes, G.A., 2007. Attachment of Shiga toxigenic *Escherichia coli* to stainless steel. Int. J. Food Microbiol 115, 89–94. https://doi.org/10.1016/j.ijfoodmicro.2006.10.027

Røder, H.L., Raghupathi, P.K., Herschend, J., Brejnrod, A., Knøchel, S., Sørensen, S.J., Burmølle, M., 2015. Interspecies interactions result in enhanced biofilm formation by co-cultures of bacteria isolated from a food processing environment. Food Microbiol. 51, 18–24. https://doi.org/10.1016/j.fm.2015.04.008

Rohman, A., Che Man, Y.B., Hashim, P., Ismail, A., 2011. FTIR spectroscopy combined with chemometrics for analysis of lard adulteration in some vegetable oils. CYTA - J. Food 9, 96–101. https://doi.org/10.1080/19476331003774639

Sánchez-Alonso, I., Carmona, P., Careche, M., 2012. Vibrational spectroscopic analysis of hake (*Merluccius merluccius L.*) lipids during frozen storage. Food Chem. 132, 160–167. https://doi.org/10.1016/j.foodchem.2011.10.047

Saubade, F., Pilkington, L.I., Liauw, C.M., Gomes, L.C., McClements, J., Peeters, M., El Mohtadi, M., Mergulhão, F.J., Whitehead, K.A., 2021. Principal component analysis to determine the surface properties that influence the self-cleaning action of hydrophobic plant leaves. Langmuir 37, 8177–8189. https://doi.org/10.1021/acs.langmuir.1c00853

Silva, E.R., Tulcidas, A.V., Ferreira, O., Bayón, R., Igartua, A., Mendoza, G., Mergulhão, F.J.M., Faria, S.I., Gomes, L.C., Carvalho, S., Bordado, J.C.M., 2021. Assessment of the environmental compatibility and antifouling performance of an innovative biocidal and foul-release multifunctional marine coating. Environ. Res. 198, 111219. https://doi.org/10.1016/j.envres.2021.111219

Skovager, A., Whitehead, K., Wickens, D., Verran, J., Ingmer, H., Arneborg, N., 2013. A comparative study of fine polished stainless steel, TiN and TiN/Ag surfaces: adhesion and attachment strength of *Listeria monocytogenes* as well as antilisterial effect. Colloids Surf. B Biointerfaces 109, 190–196. https://doi.org/10.1016/j.colsurfb.2013.03.044

Timonen, J.V.I., Latikka, M., Ikkala, O., Ras, R.H.A., 2013. Free-decay and resonant methods for investigating the fundamental limit of superhydrophobicity. Nat. Commun. 4, 2398. https://doi.org/10.1038/ncomms3398

van der Mei, H.C., de Soet, J.J.J., de Graaff, Jd, Rouxhet, P.G., Busscher, H.J., 1991. Comparison of the physicochemical surface properties of *Streptococcus rattus* with those of other mutans streptococcal species. Caries Res. 25, 415–423. https://doi.org/10.1159/000261404

van Oss, C.J., 1995. Hydrophobicity of biosurfaces - Origin, quantitative determination and interaction energies. Colloids Surf. B, Biointerfaces 5, 91–110. https://doi.org/10.1016/0927-7765(95)01217-7

Verran, J., Packer, A., Kelly, P., Whitehead, K.A., 2010. The retention of bacteria on hygienic surfaces presenting scratches of microbial dimensions. Lett. Appl. Microbiol. 50, 258–263. https://doi.org/10.1111/j.1472-765X.2009.02784.x

Vorobii, M., Teixeira-Santos, R., Gomes, L.C., Garay-Sarmiento, M., Wagner, A.M., Mergulhão, F.J., Rodriguez-Emmenegger, C., 2022. Oriented immobilization of Pep19-2.5 on antifouling brushes suppresses the development of *Staphylococcus aureus* biofilms. Prog. Org. Coat. 163, 106609. https://doi.org/10.1016/j.porgcoat.2021.106609

Wenzel, R.N., 1949. Surface roughness and contact angle. J. Phys. Colloid Chem. 53, 1466–1467. https://doi.org/10.1021/j150474a015

Whitehead, K.A., Colligon, J., Verran, J., 2005. Retention of microbial cells in substratum surface features of micrometer and sub-micrometer dimensions. Colloids Surf. B Biointerfaces 41, 129–138.

Whitehead, K.A., Olivier, S., Benson, P.S., Arneborg, N., Verran, J., Kelly, P., 2015. The effect of surface properties of polycrystalline, single phase metal coatings on bacterial retention. Int. J. Food Microbiol. 197, 92–97. https://doi.org/10.1016/j.ijfoodmicro.2014.12.030

Xu, W., Leeladhar, R., Kang, Y.T., Choi, C.-H., 2013. Evaporation kinetics of sessile water droplets on micropillared superhydrophobic surfaces. Langmuir 29, 6032–6041. https://doi.org/10.1021/la400452e

Zhao, L., Chen, R., Lou, L., Jing, X., Liu, Q., Liu, J., Yu, J., Liu, P., Wang, J., 2020. Layer-by-layer-assembled antifouling films with surface microtopography inspired by *Laminaria japonica*. Appl. Surf. Sci. 511, 145564. https://doi.org/10.1016/j.apsusc.2020.145564

Zhao, W., Wang, L., Xue, Q., 2010. Fabrication of low and high adhesion hydrophobic AU surfaces with micro/nano-biomimetic structures. J. Phys. Chem. C 114, 11509–11514. https://doi.org/10.1021/jp102052e

Zhu, Z., Zhang, Y., Sun, D.-W., 2021. Biomimetic modification of freezing facility surfaces to prevent icing and frosting during freezing for the food industry. Trends Food Sci. Technol. 111, 581–594. https://doi.org/10.1016/j.tifs.2021.02.034

Zouaghi, S., Bellayer, S., Thomy, V., Dargent, T., Coffinier, Y., Andre, C., Delaplace, G., Jimenez, M., 2019. Biomimetic surface modifications of stainless steel targeting dairy fouling mitigation and bacterial adhesion. Food Bioprod. Process. 113, 32–38. https://doi.org/10.1016/j.fbp.2018.10.012

Zouaghi, S., Six, T., Bellayer, S., Moradi, S., Hatzikiriakos, S.G., Dargent, T., Thomy, V., Coffinier, Y., André, C., Delaplace, G., Jimenez, M., 2017. Antifouling biomimetic liquid-infused stainless steel: application to dairy industrial processing. ACS Appl. Mater. Interfaces 9, 26565–26573. https://doi.org/10.1021/acsami.7b06709

Zoueki, C.W., Tufenkji, N., Ghoshal, S., 2010. A modified microbial adhesion to hydrocarbons assay to account for the presence of hydrocarbon droplets. J. Colloid Interface Sci. 344, 492–496. https://doi.org/10.1016/j.jcis.2009.12.043